Intercellular calcium signaling mediated by point-source burst release of ATP

Gregory Arcuino, Jane H.-C. Lin, Takahiro Takano, Collins Liu, Li Jiang, Qun Gao, Jian Kang, and Maiken Nedergaard*

Department of Cell Biology, Anatomy, and Pathology, New York Medical College, Valhalla, NY 10595

Edited by Michael V. L. Bennett, Albert Einstein College of Medicine, Bronx, NY, and approved May 31, 2002 (received for review November 2, 2001)

Calcium signaling, manifested as intercellular waves of rising cytosolic calcium, is, in many cell types, the result of calcium-induced secretion of ATP and activation of purinergic receptors. The mechanism by which ATP is released has hitherto not been established. Here, we show by real-time bioluminescence imaging that ATP efflux is not uniform across a field of cells but is restricted to brief, abrupt point-source bursts. The ATP bursts emanate from single cells and manifest the transient opening of nonselective membrane channels, which admits fluorescent indicators of ≤1.5 kDa. These observations challenge the existence of regenerative ATP release, because ATP efflux is finite and restricted to a point source. Transient efflux of cytosolic nucleotides from a subset of cells may represent a conserved pathway for coordinating local activity of electrically nonexcitable cells, because identical patterns of ATP release were identified in human astrocytes, endothelial cells, and bronchial epithelial cells.

Elevations in cytosolic-free calcium constitute one of the most widespread and conserved mechanisms by which hormones and transmitters regulate cell functions (1). Calcium responses often spread to surrounding cells, and calcium waves have been identified in most cell types studied, including astrocytes, bronchial epithelial cells, myocytes, endothelial cells, hepatocytes, mast cells, and pancreatic acinar cells (2–8), suggesting that this means of intercellular communication is both ubiquitous among tissues and conserved across phylogeny. Although several lines of evidence support a key role for purinergic receptors in cell–cell signaling, the mechanism by which ATP is released has not yet been established (9–11). In this study, we have taken advantage of a newly developed technique by which extracellular ATP can be visualized dynamically in cultures of live cells (12, 13). We evoked spontaneous calcium waves by lowering extracellular Ca^{2+} concentration and visualized extracellular ATP dynamically by bioluminescence imaging. Our observations suggest that ATP efflux is the result of transient activation of membrane channels in those cells from which calcium waves are initiated. As a result, the spatial expansion of calcium waves can be explained by simple diffusion of ATP, requiring neither amplification nor regeneration for spatial expansion to proceed.

Methods

Culture and Transfection. Cortical astrocytes from 1-day-old postnatal rats were prepared and maintained as described (3). Human bronchial epithelial cells were obtained from Clonetics (San Diego). Human umbilical cord vein endothelial cells were donated by Shahin Rafii (Cornell University Medical College, New York, NY; ref. 14), and adult human astrocytes by Steve Goldman (Cornell University Medical College, New York, NY; ref. 15). Transfection of C6 glioma was carried out by using lipofectin as described (16).

Calcium Imaging. The cells were grown in an eight-chamber coverglass system (Lab-Tek). Confluent cultures were loaded with 10 μM fluo-3 acetomethoxyester (fluo-3 AM, Molecular Probes) for 1 h at 37°C (3). Before measurements, each chamber was washed by replacing half the bathing medium in each wash with a Ringer buffer so as not to expose the cells to the air–water interface. The buffer contained 150 mM NaCl, 1 mM K_2HPO_4, 1 mM $MgSO_4$, 1 mM $CaSO_4$, 10 mM glucose, 10 mM Hepes, and 2 mM propidium iodine at pH 7.35. Spontaneous calcium wave activity was induced by adding an equal volume of Ca^{2+}-free Ringer's solution containing 2 mM EGTA. Mechanically triggered calcium waves were induced with a glass micropipette as described (3).

ATP Measurements and Whole-Cell Recordings. Standard whole-cell recodings were obtained by using an Axopatch 200B amplifier (17). ATP release from living cells were dynamically imaged by chemiluminescence as described by Wang *et al.* (9, 12). Light production from the luciferin—luciferase reaction was captured by a liquid nitrogen-cooled charge-coupled camera (CCD; VersArray 1300B, Princeton Instruments, Trenton, NJ) with a 20× oil lens (N.A. 0.8, Olympus). Calibrations with ATP standards (50–250 nM) showed that luminescence signal (LS) was a linear function of ATP described by $LS = 0.0108 \times ATP\ (nM) + 2.6223$; $R^2 = 0.9973$. The lowest detectable ATP standard was 50 nM.

Results and Discussion

We first addressed the possibility that ATP efflux might be mediated by transient opening of channels permissive of ATP permeation. Spontaneous astrocytic calcium wave activity was initiated by lowering extracellular calcium (18). Cultures loaded with the calcium indicator fluo-3 generated radially expanding calcium waves with a radius of 215 ± 22 μm (mean ± SEM; range 81–486 μm), and a transit velocity of 21 ± 3 μm at a frequency of 0.23 ± 0.21 waves per min per 100 cells (Fig. 1*a*). Transient increases in membrane permeability to large ions were monitored by including propidium (2 mM; 562 Da) in the recording solution. Propidium is a DNA-intercalating fluorescent indicator and is excluded by viable cells with intact plasma membranes. We found that cells which triggered calcium waves consistently admitted propidium, whereas those receiving the signals did not. Propidium was first detected in the trigger cell 18 ± 3 s after wave initiation (range 0 to 42 sec, $n = 21$); this delay likely results from the necessary accumulation of sufficient DNA-bound propidium to allow detection (Fig. 1*a*). The window of permeability during which extracellular propidium was admitted was brief and not a result of cell death, in that the trigger cell excluded propidium if the indicator was added after wave initiation (1 min; $n = 8$). Mechanical stimulation, a paradigm routinely used to trigger calcium signaling, was also associated with propidium uptake (18/18). The calcium waves were mediated by ATP, because the purinergic receptor antagonists suramin (100 μM) and reactive blue (100 μM) reduced wave radius by 76 ± 4% and 81 ± 5%, respectively ($n = 10$, $P < 0.01$). Furthermore, apyrase, an enzyme that dephosphorylates nucleotide triphosphates, restricted calcium wave propagation by 57 ± 6% ($n = 12$). The frequent oscillations in astrocytic Ca^{2+}i confined to single cells

This paper was submitted directly (Track II) to the PNAS office.

Abbreviation: CDCF, dicarboxy-dichlorofluorescein.

*To whom reprint requests should be addressed. E-mail: maiken_nedergaard@nymc.edu.

 www.pnas.org/cgi/doi/10.1073/pnas.152588599

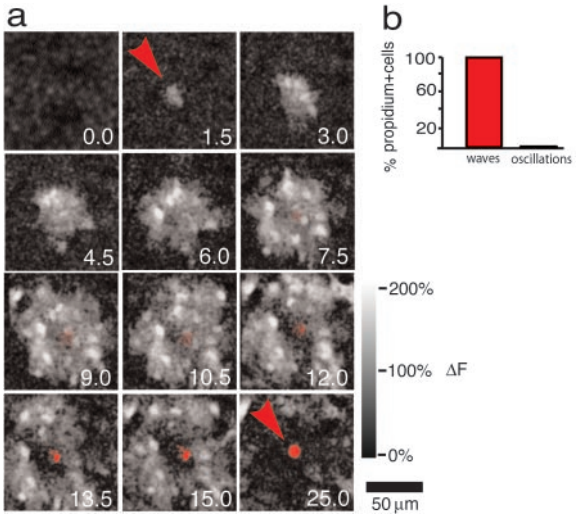

Fig. 1. Astrocytic calcium signaling is associated with a transient increase in membrane permeability and uptake of propidium. (*a*) Sequence of images (in s) demonstrating the time course of propidium uptake in the cell that triggers a calcium wave. Propidium uptake is superimposed upon a time series of confocal images displaying relative increases in fluo-3 emission (ΔF). A single cell located in the center of the calcium wave displays uptake of propidium (red arrowhead). (*b*) Histogram summarizing the fraction of cells in the center of calcium waves ($n = 21$) and cells exhibiting calcium oscillations ($n = 221$) with uptake of propidium (see supporting information, which is published on the PNAS web site, www.pnas.org).

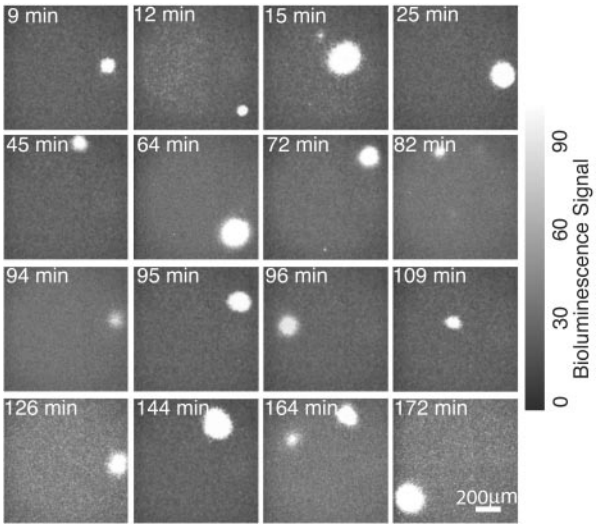

Fig. 2. ATP is released as point-source bursts. ATP release was detected as light emissions produced by ATP-triggered luciferase breakdown of luciferin. A series of bioluminescence images visualize the stochastic distribution of ATP burst releases from C6-Cx43 cells during a 3-h recording period. Bioluminescence signal is displayed in arbitrary units (see supporting information).

were, on the other hand, not associated with propidium uptake (Fig. 1*b*). Thus, increases in $Ca^{2+}i$ alone appear insufficient to initiate changes in ATP membrane permeability.

To establish a direct link between transient membrane permeability and ATP release, a mixture containing luciferase and its substrate, luciferin, was added extracellularly to cultures of rodent astrocytes. By this approach, ATP release was then monitored by light emissions resulting from ATP-triggered luciferase breakdown of luciferin. This process could be observed at the single-cell level in real time and could be assessed

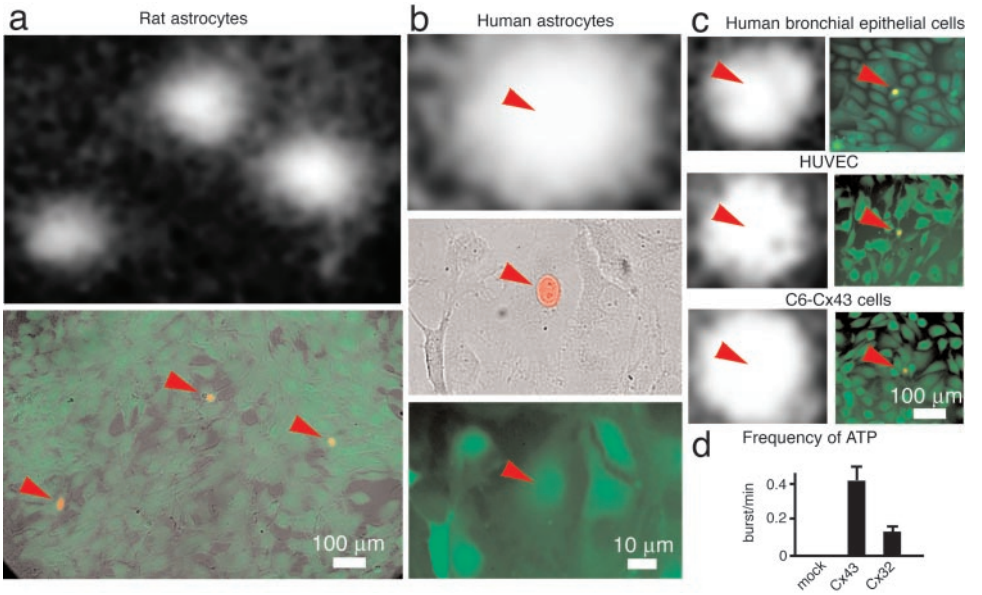

Fig. 3. ATP release is associated with a transient increase in membrane permeability and uptake of fluorescent indicators. (*A Upper*) Bioluminescence signal from three ATP burst events recorded from rat astrocytes during a 5-min period; calcein AM (1 μM) loading in the same field as *b* is shown in *Lower*. Cells in the center of ATP burst events consistently admitted propidium, indicative of a transient increase in membrane permeability. The ability of propidium$^+$ cells (red arrows) to load and retain calcein after ATP release suggests that membrane permeability was only increased transiently in cells releasing ATP. (*b*) Human astrocytes. An ATP burst event (*Top*) from a single propidium$^+$ cell (*Middle*, red arrow). The ATP-releasing cell loaded and retained calcein to a similar extent as surrounding cells (*Bottom*, red arrow). (*c*) ATP efflux (*Left*) and corresponding fields of propidium/calcein uptake in cultures of human bronchial epithelial cells, human umbilical vein endothelial cells (HUVEC), and C6 glioma cells overexpressing connexin 43 (C6-Cx43 cells). Bioluminescence signal is displayed in arbitrary units and scaled as in Fig. 1. (*d*) Comparison of the frequency of ATP burst events in C6-mock cells (Cx deficient), C6-Cx43, and C6-Cx32 cells. The frequency of ATP release is mapped as burst per min per 100 cells.

Table 1. Comparison of ATP release in the different types of cells studied

Cell type (number of experiments)	Luminescence signal* (pixel intensity)	Mean diameter† (μm)	Frequency‡ (burst/min/100 cells)
human bronchial epith (20)	62 ± 6	96 ± 6	0.12 ± 0.02
HUVEC (11)	57 ± 6	102 ± 11	0.39 ± 0.10
human astrocytes (14)	70 ± 14	111 ± 16	0.98 ± 0.15
rat astrocytes (13)	62 ± 9	82 ± 8	0.38 ± 0.18
C6-Cx43 (39)	156 ± 16	181 ± 15	0.41 ± 0.11
C6-Cx32 (7)	48 ± 10	81 ± 11	0.13 ± 0.03
C6-mock (7)	0	0	0

*Peak luminescence signals in arbitrary intensity values.
†Maximal diameter of the burst events.
‡Relative frequency of ATP burst events per min per 100 cells.

in large numbers of cells viewed concurrently with a liquid nitrogen-cooled CCD camera (Fig. 2; refs. 12 and 13). At baseline, the vast majority of cells exhibited no photodetectable ATP release. Nonetheless, these cultures exhibited frequent, unheralded point-source bursts of light emission that appeared to reflect single-cell ATP discharges when extracellular Ca^{2+} was lowered by adding an EGTA-containing buffer. These ATP bursts were (like the Ca^{2+} waves) variable in their duration and extent of radial expansion, but were uniform in their abrupt onsets from single points stochastically distributed across the culture field (Fig. 2; see supporting information).

All astrocytic ATP burst releases were associated with propidium uptake. Propidium uptake did not result from loss of viability, because cells with propidium uptake loaded with calcein AM after recording of ATP release (Fig. 3*a*). The ability of ATP-releasing cells to load and retain calcein after recording, combined with their morphologic stability and survival thereafter, suggests that these transient increases in membrane permeability do not compromise cellular viability. Also, receptor-stimulated $Ca2^{+}$ mobilization were comparable in propidium^{+} and propidium^{-} cells (see supporting information). The relative fraction of cells that released ATP in any given condition was low; typically, 0.1 to 1 ATP burst per min was observed in a field of 100 cells (Table 1).

Next, we asked whether transient increases in membrane permeability mediate ATP release in other cell types. We found that human bronchial epithelial cells, human umbilical cord vein endothelial cells (HUVEC), and astrocytes harvested from adult human brain all released ATP in bursts from single cells (Fig. 3 *b–c*). ATP bursts were consistently associated with propidium uptake in all cell types studied (Fig. 3 *a–c*). In several experiments, it was observed that a few cells repeatedly released ATP, suggesting that cells with "pacemaker" activity may exist. Furthermore, because ATP release has been linked previously to the level of connexin expression (9), ATP release in C6 cells overexpressing connexin 43 (C6-Cx43 cells) was compared with mock-transfected cells (C6-mock cells). Although C6-Cx43 cells displayed repeated bursts of ATP release similar to those of astrocytes, no ATP bursts were observed in Cx-deficient mock-transfected (C6-mock) cells (total recording 265 min, 16 experiments, Fig. 3 *c–d*). C6 cells overexpressing another member of the Cx family, connexin 32 (C6-Cx32 cells), frequently exhibited spontaneous ATP bursts, thus supporting and extending the idea that Cx expression positively regulates ATP release (Fig. 3*d*). In addition to an increase in the number of hemichannels, overexpression of Cx43 is associated with altered expression of other genes (19) and increased cell stiffness (20). Thus, it is not possible to conclude that ATP flows out of Cx hemichannels based upon this report.

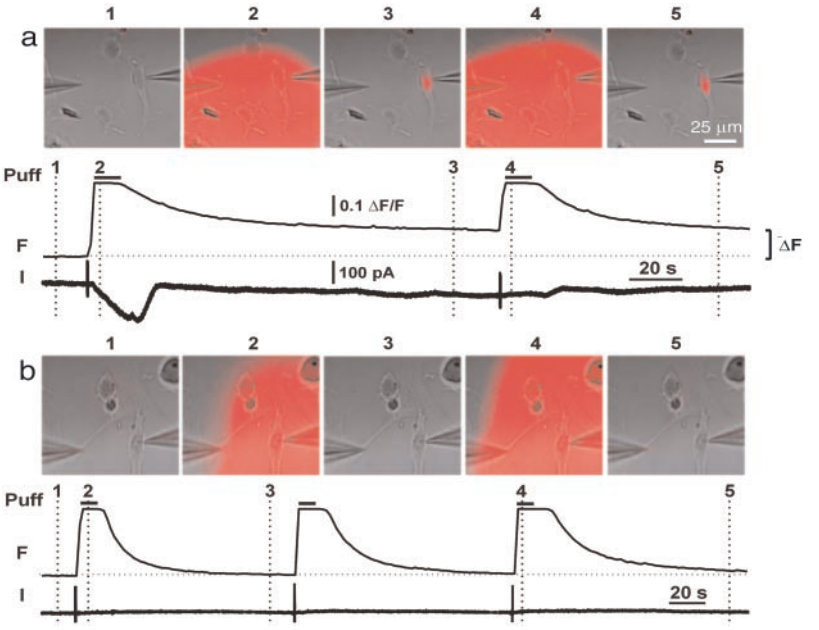

Fig. 4. Propidium influx is associated with a transient activation of an inward current in C6-Cx43 cells. (*a*) Propidium uptake and whole-cell recordings in a responding cell. A single cell was patched in the voltage-clamp configuration with a holding potential of −60 mV (right pipette). Another pipette (left) was used to apply a Ca^{2+}-free solution locally (10 mM EGTA, 2 mM propidium, 10-s pulse). (*Upper*) Sequence of images collected at indicated time displays cellular uptake of propidium evoked by local application of the Ca^{2+}-free solution. (*Lower*) Relative changes in fluorescence as a function of time (F) and whole-cell recordings (I) in the same cell. Solid bars indicate that the Ca^{2+}-free solution was applied. Uptake of propidium is detected as a relative increase in fluorescence after the first stimulation (ΔF). The first challenge with a Ca^{2+}-free solution activated an inward current, whereas neither inward current nor further propidium uptake was elicited when the stimulation was repeated. (*b*) Sequence of images illustrating a nonresponding cell. The cell excluded propidium and did not increase membrane permeability during repeated exposures to a Ca^{2+}-free solution.

To characterize the ATP permeation pathway, we combined whole-cell recordings with concurrent detection of propidium uptake. A Ca^{2+}-free solution was locally applied through a patch pipette and was associated with dye uptake in 5–10% of C6 Cx43 cells, whereas an identical application of a Ca^{2+}-containing solution did not result in propidium uptake (data not shown). Interestingly, exposure to a Ca^{2+}-free solution activated an inward current in 7.5% of the cells (10 responding cells of a total of 134 cells). Activation of the inward current closely correlated with propidium uptake, because all 10 responding cells displayed propidium uptake, whereas all 124 nonresponding cells excluded propidium (Fig. 4 *a–b*). The inward current activated with a lag-time of 7.0 ± 1.5 s (range: 1.2–12 s). The peak amplitude was 127 ± 13 pA (range: 81–220 pA) with a mean duration of 15.7 ± 2.6 s (range: 1.6–30.7 s). Assuming that the putative ATP-releasing channel has a reversal potential of 0 mV, and a single-channel conductance of 100 pS (21), an inward current of 127 pA represent about 33 open channels.

The inward current could only be activated once in responding cells, and repetitive application of the Ca^{2+}-free solution was not associated with additional propidium uptake (Fig. 3 *a–b*). The fact that channel openings only occurred in a minor fraction of the cells and could not be repetitively activated (Fig. 4*a*) complicated further characterization of the channels permeable to ATP. Nevertheless, these observations demonstrate that transmembrane influx of propidium and, thereby, ATP release (Fig. 3) occur in conjunction with a transient activation of membrane channels.

To establish the ion selectivity of the ATP-releasing channels, we next exposed C6-Cx43 cells to a Ca^{2+}-free solution in the presence of both dicarboxy-dichlorofluorescein (CDCF) (anion) and propidium (cation). Almost all propidium$^+$ cells displayed intense uptake of CDCF (Fig. 5*a*). In contrast, only 11% of the cells contained both fluorescent indicators, if propidium was applied in a Ca^{2+}-free solution and followed by CDCF. If the two dyes were sequentially applied in the opposite order, 9% of the cells contained both dyes. (Fig. 5*b*). Thus, both large anions and cations can permeate the channels, and the permeability changes are transient in the majority of the cells, because cells with CDCF uptake excluded propidium during the second stimulation. Both CDCF and propidium are gap-junction permeable. However, the high affinity of propidium to DNA effectively eliminates gap-junction diffusion, resulting in clusters of cells with CDCF surrounding single cells with uptake of both indicators. To define the upper size limit of molecules that can permeate the channels, C6-Cx43 cells next were stimulated in the presence of high molecular weight, fluorescein-conjugated dextrans. Uniformly, propidium$^+$ cells excluded all of the fluorescein-dextran conjugates studied (3.0, 10.0, and 2,000 kDa), indicating that the upper limit for fluorescent indicator uptake is below 1.5 kDa (the 3.0-kDa dextran preparation contained polymers with sizes in the range of 1.5–3.0 kDa; Fig. 5*c*). We considered the possibility that the inability to detect uptake of the high molecular weight dextrans resulted from insufficient sensitivity of our fluorescence detection system. However, application of the product obtained by treating the 3.0-kDa fluorescein-conjugated dextran with dextranase (50 units/ml) resulted in labeling of the same cells that took up propidium iodide (Fig. 5*d*), indicating that fluorescein-dextrans were excluded due to their large size. Combined with the observation that propidium influx was linked to an increase in whole-cell current (Fig. 4*a*), these data indicate that the uptake of fluorescent indicators is mediated by transient openings of channels and does not result from nonspecific membrane rupture or endocytosis. ATP bursting was not a result of cell death, because the ATP-releasing cells were able to load and retain calcein/AM (Fig. 3). As an additional measure of cell viability, we also evaluated the ability of propidium$^+$ cells to mobilize intracellular Ca^{2+} in response to purinergic-receptor stimulation. C6-Cx43 cells were exposed to a Ca^{2+}-free solution (6 min, 2 mM propidium) to trigger propidium uptake. Six hours later, the cultures were loaded with fluo-3/AM and exposed to ATP (100 μM). The peak Ca^{2+} increments in propidium$^+$ cells (218 ± 11%, n = 88) were not statistically different from the responses in neighboring propidium$^-$ cells (182 ± 9%, n = 81), indicating that propidium uptake did not compromise cell viability.

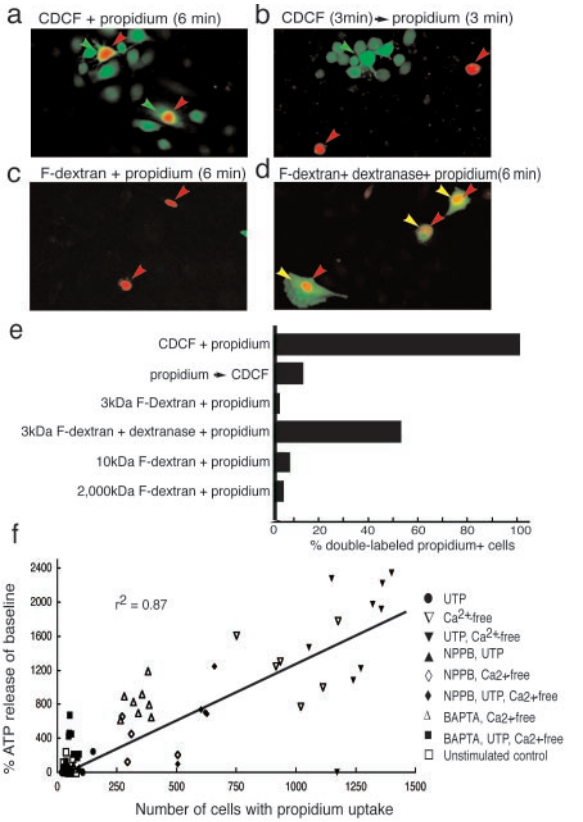

Fig. 5. The increase in membrane permeability is transient and allows influx of both cations and anions below 1.5 kDa. (*a*) CDCF (green arrowhead, 445 Da) and propidium (red arrowhead, 562 Da) were both taken up by the same cells during a 6-min exposure to a Ca^{2+}-free solution containing both indicators. CDCF is gap junction permeable, and clusters of cells with CDCF surround single cells with uptake of both indicators (red and green arrowheads). (*b*) Separate populations of cells took up the two indicators if first exposed to a Ca^{2+}-free solution containing CDCF (3 min) followed by a second exposure to a Ca^{2+}-free solution containing propidium (3 min). (*c*) Fluorescein dextran (>1.5 kDa) was excluded by cells with propidium uptake (6 min). (*d*) Dextranase digestion of the 3-kDa fluorescein-dextran conjugate resulted in uptake of the indicator in propidium$^+$ cells (yellow arrowhead; 6 min). (*e*) Histogram summarizing the percentage of propidium$^+$ cells with uptake of CDCF or fluorescein dextran. (*f*) ATP release as a function of the total number of cells with propidium uptake in the same culture. ATP release is plotted as a percentage of baseline (unstimulated) release from the same culture. Each culture contained a total of ≈16,000 cells.

To compare ATP secretion on a larger scale with transient changes in membrane permeability, ATP release was correlated with the total number of cells with propidium uptake in the same culture. Confluent C6-Cx43 cell cultures were stimulated by exposure to a Ca^{2+}-free solution, UTP (100 μM), or a combination of both. We observed that ATP release increased as a function of cells with propidium uptake. The chloride channel blocker, NPPB, or chelating cytosolic Ca^{2+} with 1,2-bis(2-aminophenoxy)ethane-*N,N,N′,N′*-tetraacetate/acetoxymethyl ester (BAPTA/AM), both reduced ATP release and propidium uptake in parallel (Fig. 5*e*). Because ATP release was a direct

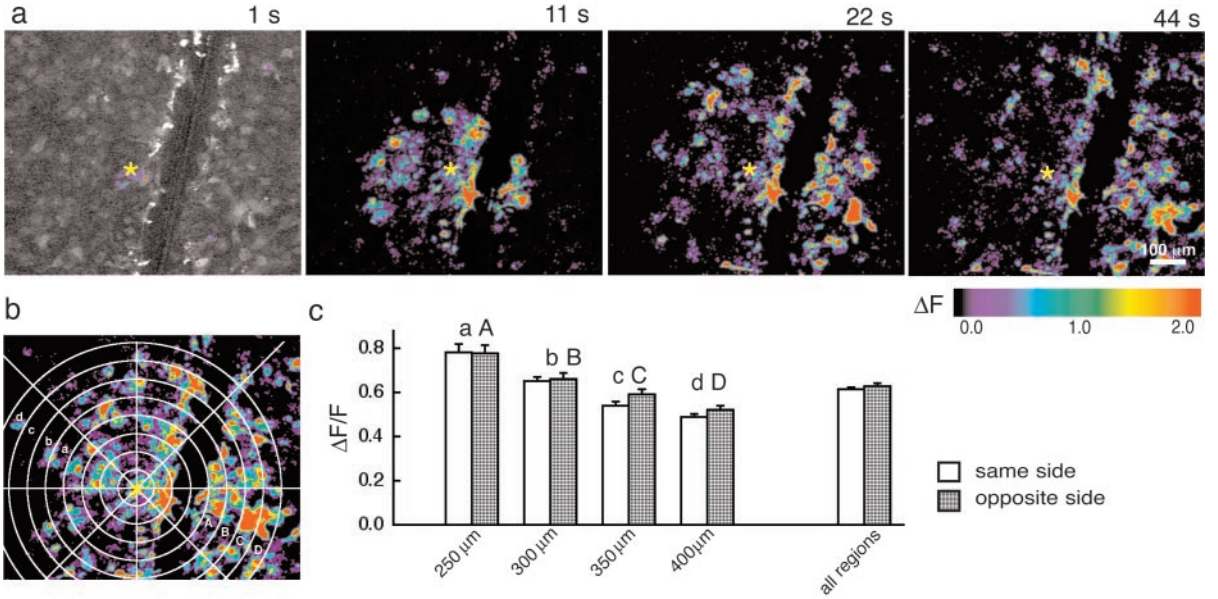

Fig. 6. The effect of a cell-free lane on mechanically induced astrocytic calcium signaling. (*a*) Sequential expansion of a calcium wave (1–44 s). The calcium wave was evoked on the left side of a cell-free lane (*). Relative increase in Ca^{2+}i (ΔF) was superimposed upon a fluo-3 image collected before stimulation. (*b*) Grid used for quantification of ΔF. The grid was positioned with its center on top of the stimulation site and consisted of concentric rings each with a width of 50 μm. ΔF was calculated in these radially defined sections (a, b, c, d) and compared with matching regions on the opposite side of the cell-free lane (A, B, C, D). (*c*) Histogram comparing ΔF in matched sections at increasing distance from the point of stimulation (n = 44–67). ''All regions'' indicates ΔF (mean ± SEM) in a total of 242 matched regions analyzed. No difference between regions on either side of the cell-free lane was evident.

function of propidium$^+$ cells, these data support the notion that the primary, and possibly the only, mechanism of ATP release is transient increases in membrane permeability that takes place in 0.1–1.0% of the total population of cells during a 6-min period. It is unclear why only a fraction of the cells increased membrane permeability upon stimulation (22, 23). High cytosolic Ca^{2+} levels appear to play a role, because BAPTA loading decreased both dye uptake and ATP release (Fig. 5*e*). Many cells, including astrocytes, possess a Ca^{2+}-sensing mechanism by which cytosolic Ca^{2+} concentration increases in response to low extracellular Ca^{2+} (18). In isolation, increments in cytosolic Ca^{2+} were not sufficient for channel opening, because Ca^{2+} oscillations were not associated with dye uptake (Fig. 1*b*). Molecular identification of the channels permeable to ATP and a detailed study of their gating characteristics are clearly needed.

The fact that only the cells that trigger calcium waves (Fig. 1) were propidium$^+$ does not exclude the possibility that neighboring cells release additional ATP, because less robust membrane permeabilization changes may reduce propidium uptake below detection. As an alternative approach to test whether ATP is secreted in a regenerative pattern during wave propagation, we analyzed the effect of cell-free areas on signaling expansion. Cell-free lanes with an average width of 105 ± 8 μm were produced by cutting confluent cultures of astrocytes with a scalpel blade and then allowing 6–8 h for recovery. This approach was originally used to show that an extracellular factor contributes to calcium wave propagation, because the calcium wave could ''jump'' across a cell-free lane (ref. 24; Fig. 6*a*). The probability of engaging in the calcium wave on either side of the lane was analyzed by comparing calcium responses in concentric sections placed symmetrically around the point of stimulation but on opposite sides of the cell-free lane (Fig. 6*b*). No significant difference in calcium increments was evident when comparing a total of 242 matching sections on either side of the scrape (Fig. 6*c*). Thus, cells that were physically isolated were just as likely to engage in calcium signaling as were cells linked by neighboring cells to the stimulated cell. These data argue that ATP is released from a point source and that neighboring cells receive, but do not actively contribute to the propagation of the wave. In addition, these data support the notion that gap junction-mediated diffusion plays only a minor role, if any, in calcium waves. It is important to note, that the lack of a regenerative step does not decrease the biological significance of this signaling pathway. In essence, point-source ATP bursts can be regarded as a mechanism of local signaling by which a stimulated cell can increase cytosolic Ca^{2+} in neighboring cells. Our observations do not exclude the existence of regenerative calcium waves in other systems. For example, gap junctions may play a role in paracrine signaling in the ocular ciliary epithelium and in the anterior pituitary (25, 26). In brain, ATP is a potential paracrine transmitter between electrically excitable and nonexcitable cells, because purinergic receptors are expressed by nonneuronal cells, including astrocytes, endothelial, and microglial cells, in addition to neurons (11, 13).

ATP-mediated signaling events are of particular importance in human airway epithelial cells, where P2Y receptors control several steps of mucociliary clearance by promoting Cl^- secretion and ciliary beating (27). Dysfunction of ATP-activated pathways contributes to the pathogenesis of cystic fibrosis, in that the CFTR facilitates ATP release (28). However the route of ATP release has been unclear because multiple investigators have failed to demonstrate conclusively the existence of ATP-permeable channels (29, 30). In the context of our current findings, this is understandable, because the likelihood of patching an ATP-releasing cell is small, given the stochastic distribution and transient nature of ATP release among cells within a culture. Thus, our observation that ATP is released in burst-like events from single cells may explain why it has proven difficult to obtain reliable recordings of ATP-permeable channels.

It has been recognized for decades that, in addition to its role in energy metabolism, ATP also operates as an intercellular transmitter by activation of purinergic receptors (31). The conceptual message of our study is that ATP release is mediated by transient increases in membrane permeability, and that efflux

of cytosolic ATP thereby serves as a simple signaling tool among nonexcitable cells. ATP is highly concentrated in the cytosol (≈2 mM), and efflux of ATP from a single cell has the potential to activate several hundred neighboring cells. As such, the ability of individual cells transiently to increase membrane permeability to nucleotides provides a mechanism for rapid coordination of cell activity in multicellular tissue. ATP may exit through the opening of unapposed Cx hemichannels, because Cx expression is associated with an increased potential for ATP release, and because lowering of extracellular Ca^{2+} opens Cx hemichannels (22, 23). A recent study found that metabolic inhibition was associated with membrane permeabilization of wild-type astrocytes, whereas astrocytes from Cx-deficient mice excluded fluorescent indicators (32). The collapse of electrochemical gradient in stroke may thereby result from Cx43-hemichannel opening. Because ischemia leads to an abrupt decline in extracellular Ca^{2+} from 2 mM to ≈0.2 mM, a mechanism similar to that studied here may be involved in anoxic depolarization (32, 33).

We thank Steve Goldman and Bill Ross for their critical review of this manuscript and Dhanonjoy C. Saha for helpful suggestions with the statistical analysis. This work was supported by National Institutes of Health/National Institute of Neurological Disorders and Stroke Grants NS30007 and NS38073 (to M.N.) and NS37349 (to J.K.).

1. Berridge, M. J. (1997) *J. Physiol.* **499,** 291–306.
2. Cornell-Bell, A. H., Finkbeiner, S. M., Cooper, M. S. & Smith, S. J. (1990) *Science* **247,** 470–473.
3. Nedergaard, M. (1994) *Science* **263,** 1768–1771.
4. Patel, S., Robb-Gaspers, L. D., Stellato, K. A., Shon, M. & Thomas, A. P. (1999) *Nat. Cell Biol.* **1,** 467–471.
5. Kaneko, T., Tanaka, H., Oyamada, M., Kawata, S. & Takamatsu, T. (2000) *Circ. Res.* **86,** 1093–1099.
6. Walsh, D. E., Harvey, B. J. & Urbach, V. (2000) *J. Membr. Biol.* **177,** 209–219.
7. Osipchuk, Y. & Cahalan, M. (1992) *Nature (London)* **359,** 241–244.
8. Bertuzzi, F., Davalli, A. M., Nano, R., Socci, C., Codazzi, F., Fesce, R., Di Carlo, V., Pozza, G. & Grohovaz, F. (1999) *Diabetes* **48,** 1971–1978.
9. Cotrina, M. L., Lin, J. H., Alves-Rodrigues, A., Liu, S., Li, J., Azmi-Ghadimi, H., Kang, J., Naus, C. C. & Nedergaard, M. (1998) *Proc. Natl. Acad. Sci. USA* **95,** 15735–15740.
10. Guthrie, P. B., Knappenberger, J., Segal, M., Bennett, M. V., Charles, A. C. & Kater, S. B. (1999) *J. Neurosci.* **19,** 520–528.
11. Fields, R. D. & Stevens, B. (2000) *Trends Neurosci.* **23,** 625–633.
12. Wang, Z., Haydon, P. G. & Yeung, E. S. (2000) *Anal. Chem.* **72,** 2001–2007.
13. Newman, E. A. (2001) *J. Neurosci.* **21,** 2215–2223.
14. Peichev, M., Naiyer, A. J., Pereira, D., Zhu, Z., Lane, W. J., Williams, M., Oz, M. C., Hicklin, D. J., Witte, L., Moore, M. A. & Rafii, S. (2000) *Blood* **95,** 952–958.
15. Roy, N. S., Wang, S., Jiang, L., Kang, J., Benraiss, A., Harrison-Restelli, C., Fraser, R. A., Couldwell, W. T., Kawaguchi, A., Okano, H., *et al*. (2000) *Nat. Med.* **6,** 271–277.
16. Lin, J. H., Weigel, H., Cotrina, M. L., Liu, S., Bueno, E., Hansen, A. J., Hansen, T. W., Goldman, S. & Nedergaard, M. (1998) *Nat. Neurosci.* **1,** 494–500.
17. Kang, J., Jiang, L., Goldman, S. A. & Nedergaard, M. (1998) *Nat. Neurosci.* **1,** 683–692.
18. Zanotti, S. & Charles, A. (1997) *J. Neurochem.* **69,** 594–602.
19. Naus, C. C., Bond, S. L., Bechberger, J. F. & Rushlow, W. (2000) *Brain Res. Brain Res. Rev.* **32,** 259–266.
20. Quist, A. P., Rhee, S. K., Lin, H. & Lal, R. (2000) *J. Cell Biol.* **148,** 1063–1074.
21. Bukauskas, F. F., Bukauskiene, A., Bennett, M. V. L. & Verselis, V. K. (2001) *Biophys. J.* **81,** 137–152.
22. Kondo, R. P., Wang, S. Y., John, S. A., Weiss, J. N. & Goldhaber, J. I. (2000) *J. Mol. Cell. Cardiol.* **32,** 1859–1872.
23. Li, H., Liu, T. F., Lazrak, A., Peracchia, C., Goldberg, G. S., Lampe, P. D. & Johnson, R. G. (1996) *J. Cell Biol.* **134,** 1019–1030.
24. Hassinger, T. D., Guthrie, P. B., Atkinson, P. B., Bennett, M. V. L. & Kater, S. B. (1996) *Proc. Natl. Acad. Sci. USA* **93,** 13268–13273.
25. Hirata, K., Nathanson, M. H. & Sears, M. L. (1998) *Proc. Natl. Acad. Sci. USA* **95,** 8381–8386.
26. Fauquier, T., Guerineau, N. C., McKinney, R. A., Bauer, K. & Mollard, P. (2001) *Proc. Natl. Acad. Sci. USA* **98,** 8891–8896.
27. Schwiebert, E. M., Egan, M. E., Hwang, T. H., Fulmer, S. B., Allen, S. S., Cutting, G. R. & Guggino, W. B. (1995) *Cell* **81,** 1063–1073.
28. Cantiello, H. F., Jackson, G. R., Jr., Grosman, C. F., Prat, A. G., Borkan, S. C., Wang, Y., Reisin, I. L., O'Riordan, C. R. & Ausiello, D. A. (1998) *Am. J. Physiol.* **274,** C799–C809.
29. Grygorczyk, R., Tabcharani, J. A. & Hanrahan, J. W. (1996) *J. Membr. Biol.* **151,** 139–148.
30. Reddy, M. M., Quinton, P. M., Haws, C., Wine, J. J., Grygorczyk, R., Tabcharani, J. A., Hanrahan, J. W., Gunderson, K. L. & Kopito, R. R. (1996) *Science* **271,** 1876–1879.
31. Guidotti, G. (1996) *Chem. Biol.* **3,** 703–706.
32. Contreras, J. E., Sanchez, H. A., Eugenin, E. A., Speidel, D., Theis, M., Willecke, K., Bukauskas, F. F., Bennett, M. V. L. & Saez, J. C. (2002) *Proc. Natl. Acad. Sci. USA* **99,** 495–500.
33. Hansen, A. J. & Nedergaard, M. (1988) *Neurochem. Pathol.* **9,** 195–209.